



*Liberté
Égalité
Fraternité*



Simulation of electric discharges on the solar panels of satellites

Capucine SOL¹, Sébastien Hess¹, Julien Jarrige¹, Carla Costa²

MeVArc – June 4th 2025

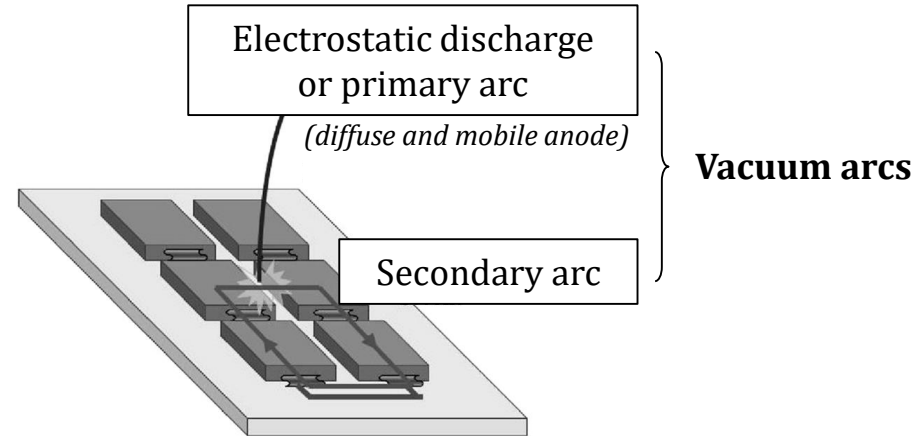
¹ONERA The French Aerospace Lab, DPHY/CSE, 2 ave M. Pélegrin 31400 Toulouse, France

²CNES, 18 Ave E. Belin 31400 Toulouse, France

Simulation of electric discharges on the solar panels of satellites



The **space environment** charges the satellite

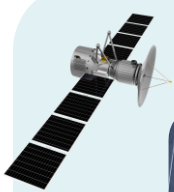


Schematic picture of a **primary arc** and a **secondary arc**

M. Cho, T. Kitamura, H. Masui and K. Toyoda *J. Spacecr. Rockets*, vol. 46, n° 2, p. 438-448, 2009

Summary

Physical mechanisms at work



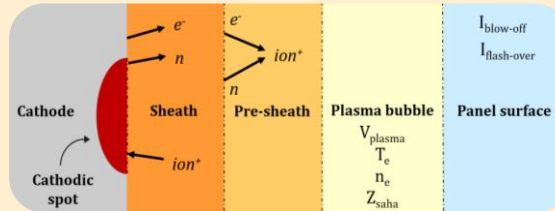
Charge and discharge of the solar panels of satellites



Material consequences of secondary arcing on a solar cell (ONERA)

Numerical model

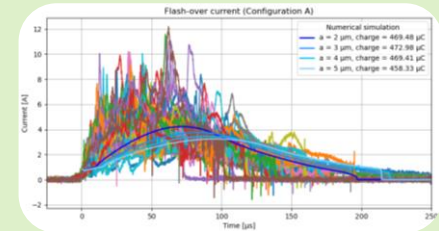
Numerical model of discharge : from the cathodic spot to the panel's surface



Schematic layout of the discharge numerical model

Results & Discussion

Comparison of numerical and experimental results



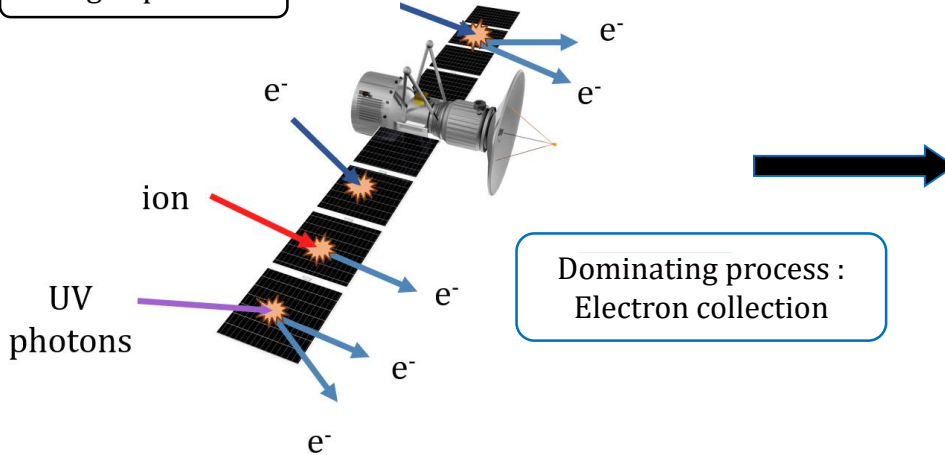
Neutralization current collected on a solar panel

Physical mechanisms - Satellite charging in space

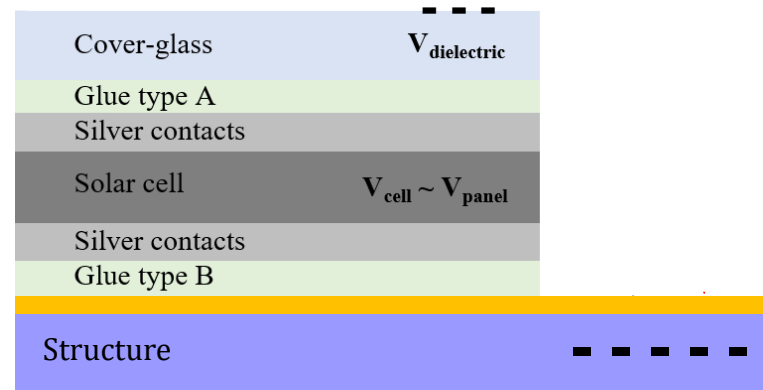
Satellite & space environment interactions lead to **charging**

$$V_{\text{env}} = 0 \text{ V}$$

Charged particles



Interactions at the surface of a satellite in orbit



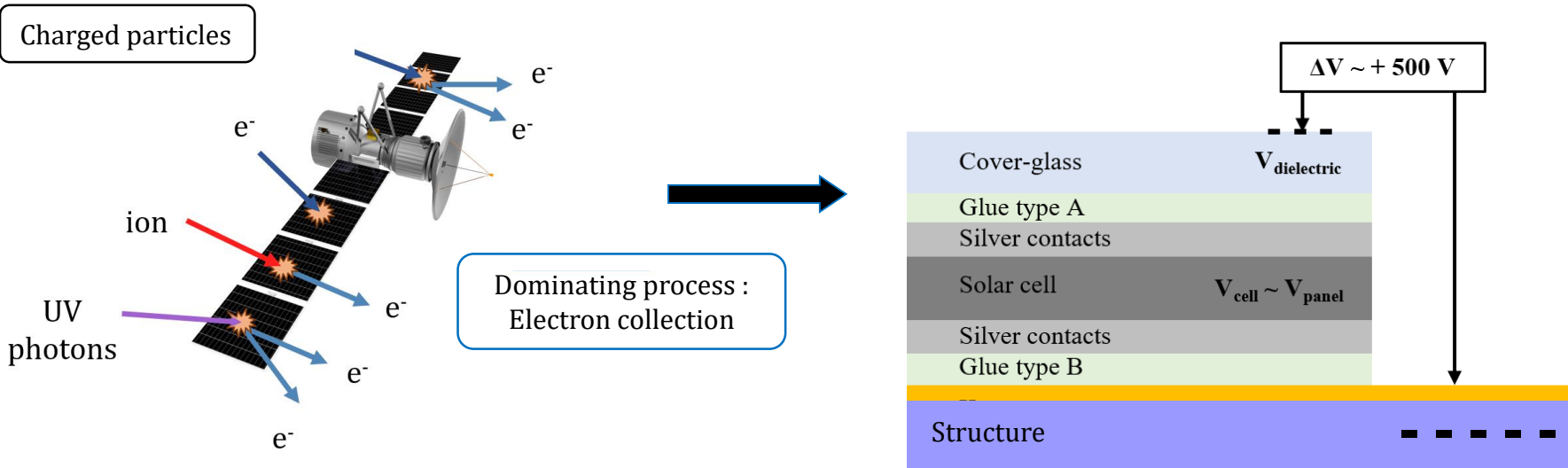
Potential differences caused by differential charging

H. Masui, T. Ose, T. Kitamura, K. Toyoda, et M. Cho *J. Spacecr. Rockets*, vol. 47, n° 6, p. 966-973, 2010

Physical mechanisms - Satellite charging in space

Satellite & space environment interactions lead to **charging**

$$V_{\text{env}} = 0 \text{ V}$$



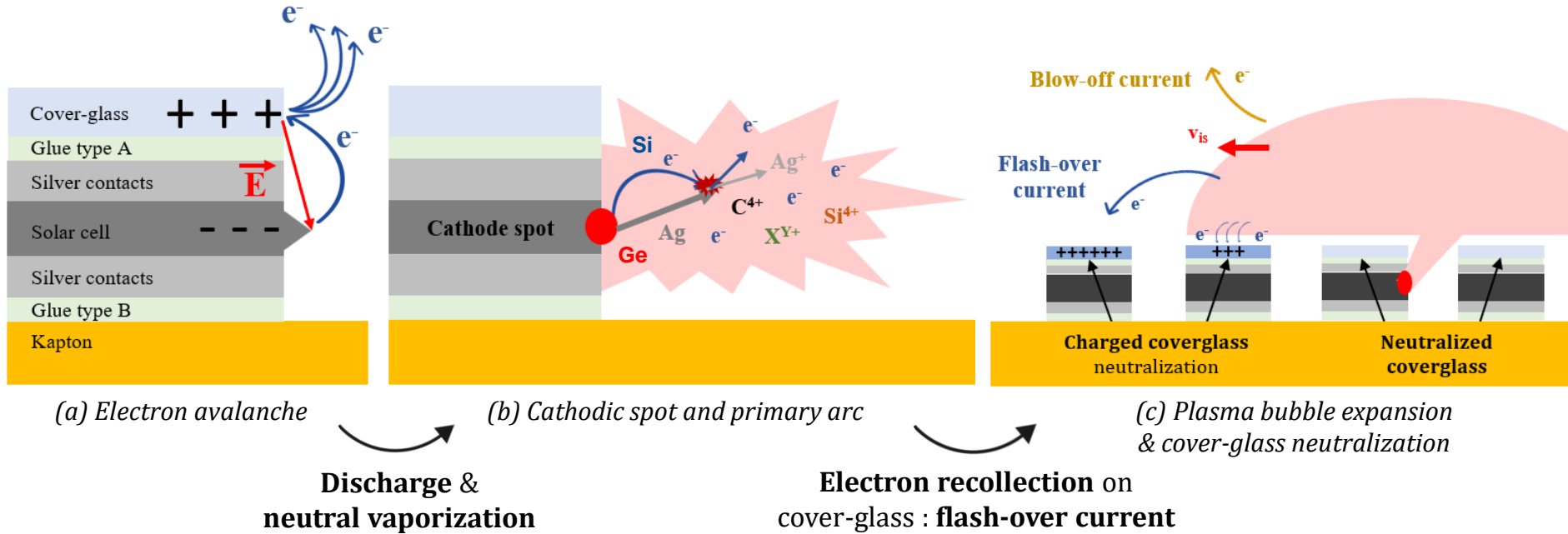
Interactions at the surface of a satellite in orbit

Potential differences caused by differential charging

H. Masui, T. Ose, T. Kitamura, K. Toyoda, et M. Cho *J. Spacecr. Rockets*, vol. 47, n° 6, p. 966-973, 2010

Physical mechanisms – Electrostatic discharge (ESD) formation

Mecanisms leading to the **formation of an electrostatic discharge** on the satellite's solar panel

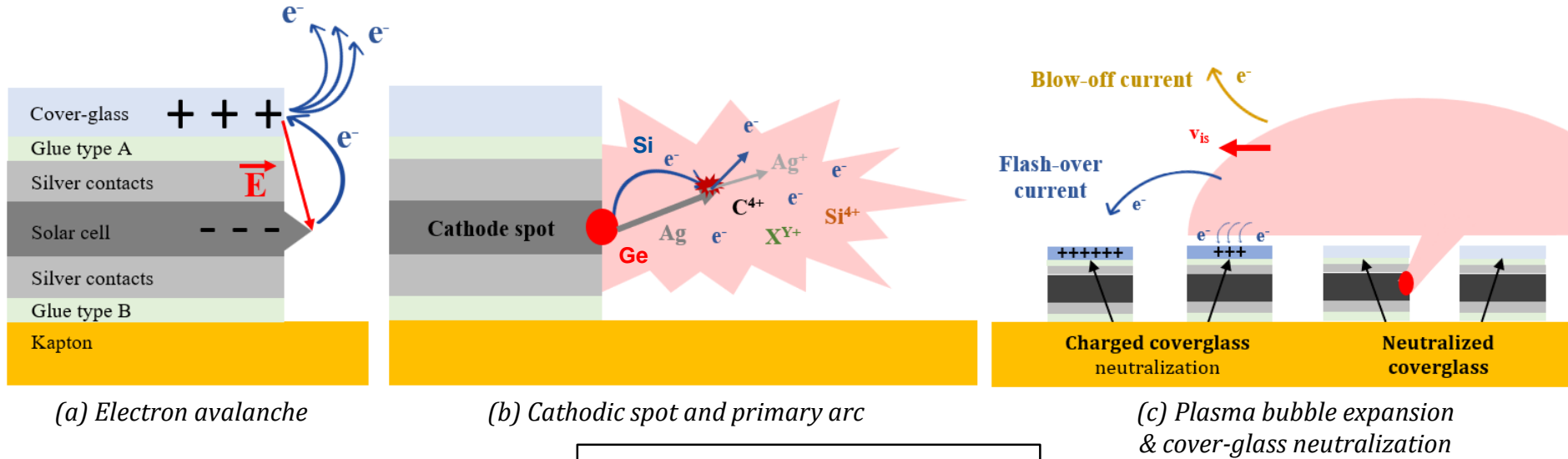


P. Sarrailh et al., IEEE Trans. Plasm. Sci. 41, 12 (2013)

H. Masui, T. Ose, T. Kitamura, K. Toyoda, et M. Cho J. Spacecr. Rockets, vol. 47, n° 6, p. 966-973, 2010

Physical mechanisms – Electrostatic discharge (ESD) formation

Mecanisms leading to the **formation of an electrostatic discharge** on the satellite's solar panel



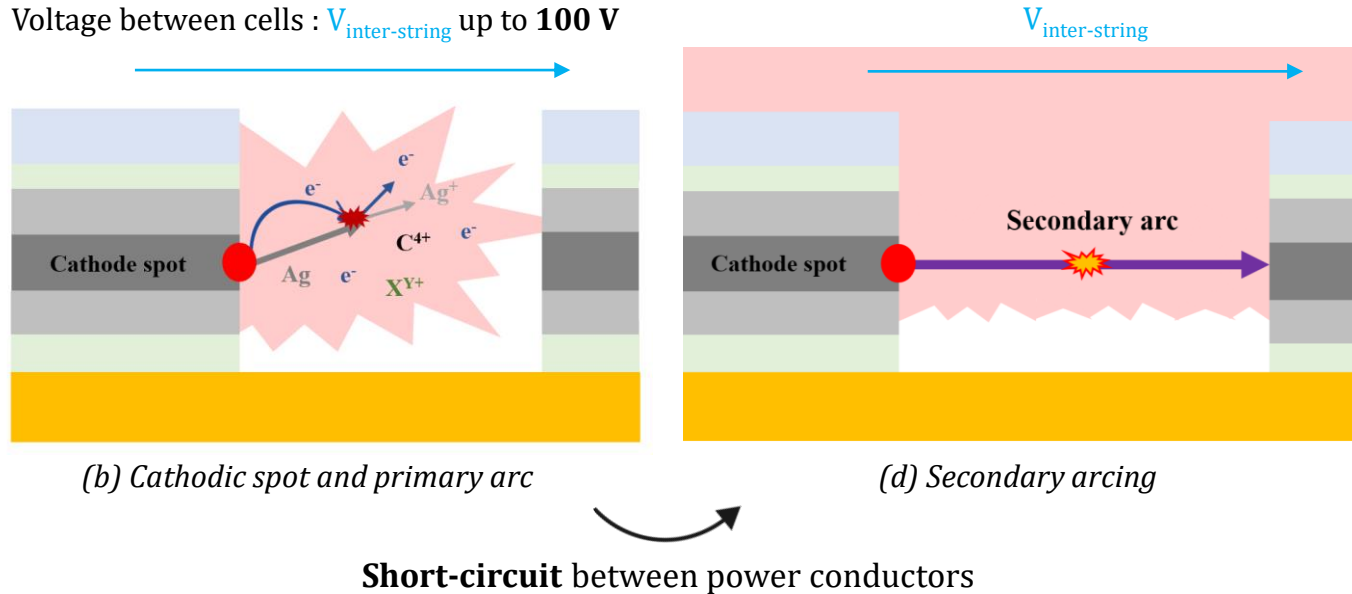
8 m² solar panel
(standard solar array) $\left\{ \begin{array}{l} I_{FO} \sim \text{a few A} \\ \tau \sim 500 \mu\text{s} \end{array} \right.$

P. Sarrailh et al., IEEE Trans. Plasm. Sci. 41, 12 (2013)

H. Masui, T. Ose, T. Kitamura, K. Toyoda, et M. Cho J. Spacecr. Rockets, vol. 47, n° 6, p. 966-973, 2010

Physical mechanisms – Secondary arc formation

Mecanisms leading to **secondary arcing** on the satellite's solar panel



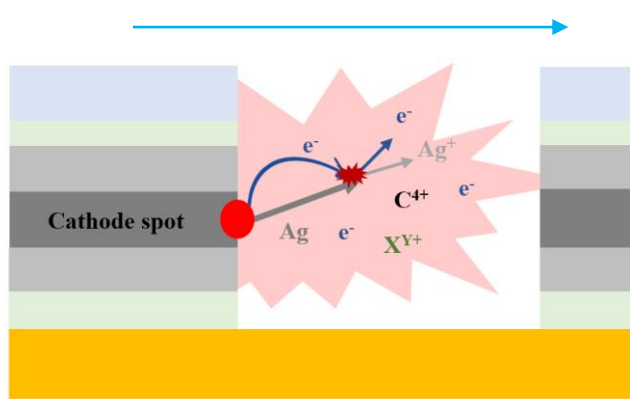
P. Sarrailh et al., IEEE Trans. Plasm. Sci. 41, 12 (2013)

H. Masui, T. Ose, T. Kitamura, K. Toyoda, et M. Cho J. Spacecr. Rockets, vol. 47, n° 6, p. 966-973, 2010

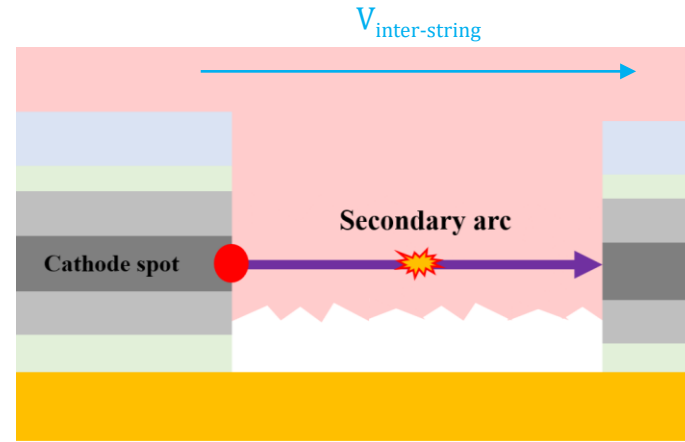
Physical mechanisms – Secondary arc formation

Mecanisms leading to **secondary arcing** on the satellite's solar panel

Voltage between cells : $V_{\text{inter-string}}$ up to **100 V**



(b) Cathodic spot and primary arc



(d) Secondary arcing

$$\text{Secondary arc} \left\{ \begin{array}{l} I_{\text{arc}} \sim \mathbf{1-3 \text{ A}} \\ \tau \sim \text{from } \mathbf{500 \mu\text{s}} \text{ (primary arc) to ? (sustained arc)} \end{array} \right.$$

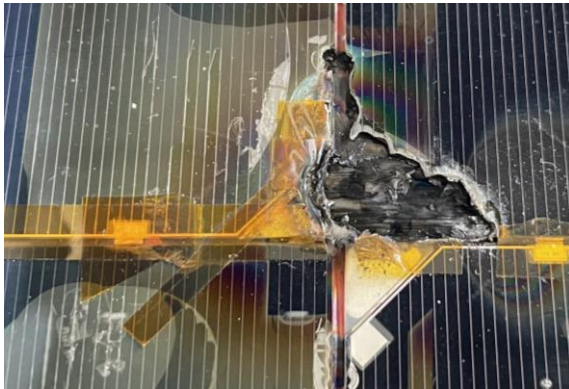
P. Sarrailh et al., IEEE Trans. Plasm. Sci. 41, 12 (2013)

H. Masui, T. Ose, T. Kitamura, K. Toyoda, et M. Cho J. Spacecr. Rockets, vol. 47, n° 6, p. 966-973, 2010

Physical mechanisms – Secondary arc, risks and stakes

Secondary arcing **risks**

Material degradation (solar cells)
Significant power loss (Midori-2, 2003)
Electromagnetic compatibility

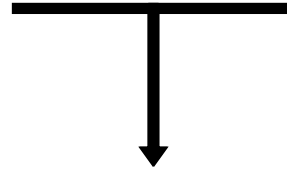


Example of cell degradation after a 1 ms secondary arc (ONERA)

Secondary arcing **stakes**

Panel size
Available onboard power ~ 10 kW
Interstring voltage ~ 100-200 V

Growing demand of communication capacity



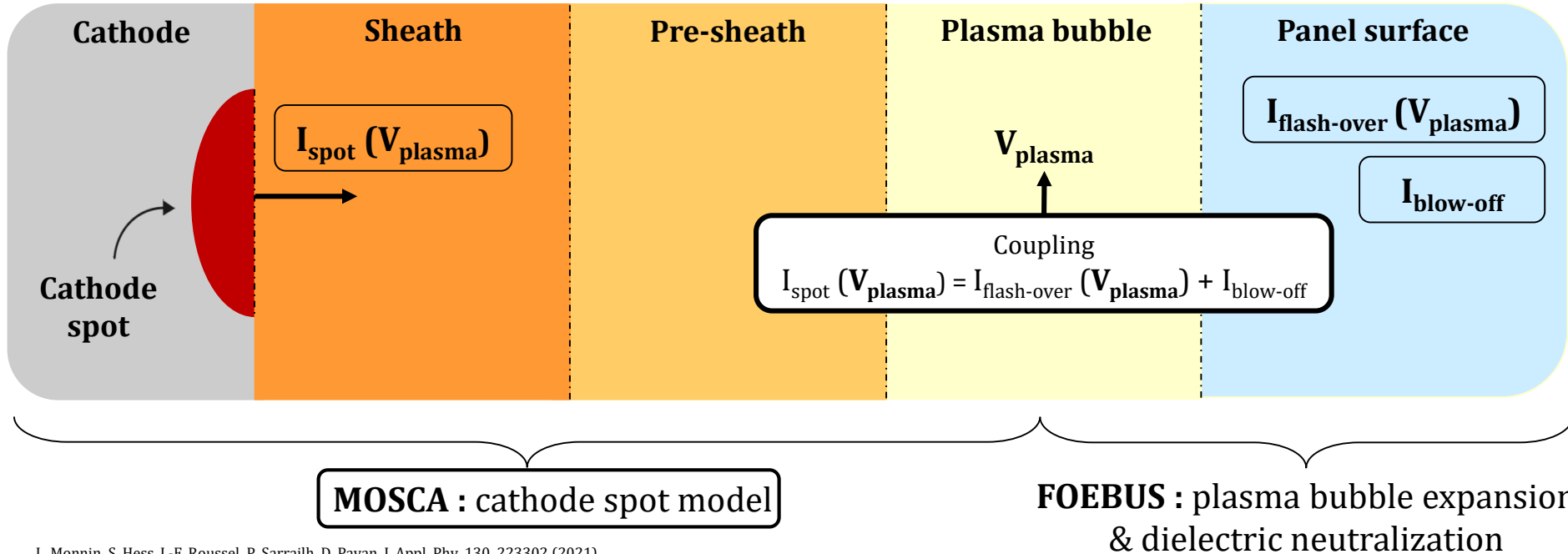
At ONERA

Experiments :
Solar panel **qualification**
test **campaigns** & ESD
characterization

Numerical simulation :
Electrostatic discharge
model from cathodic spot
to discharge panel

Numerical model – Electrostatic discharge global model

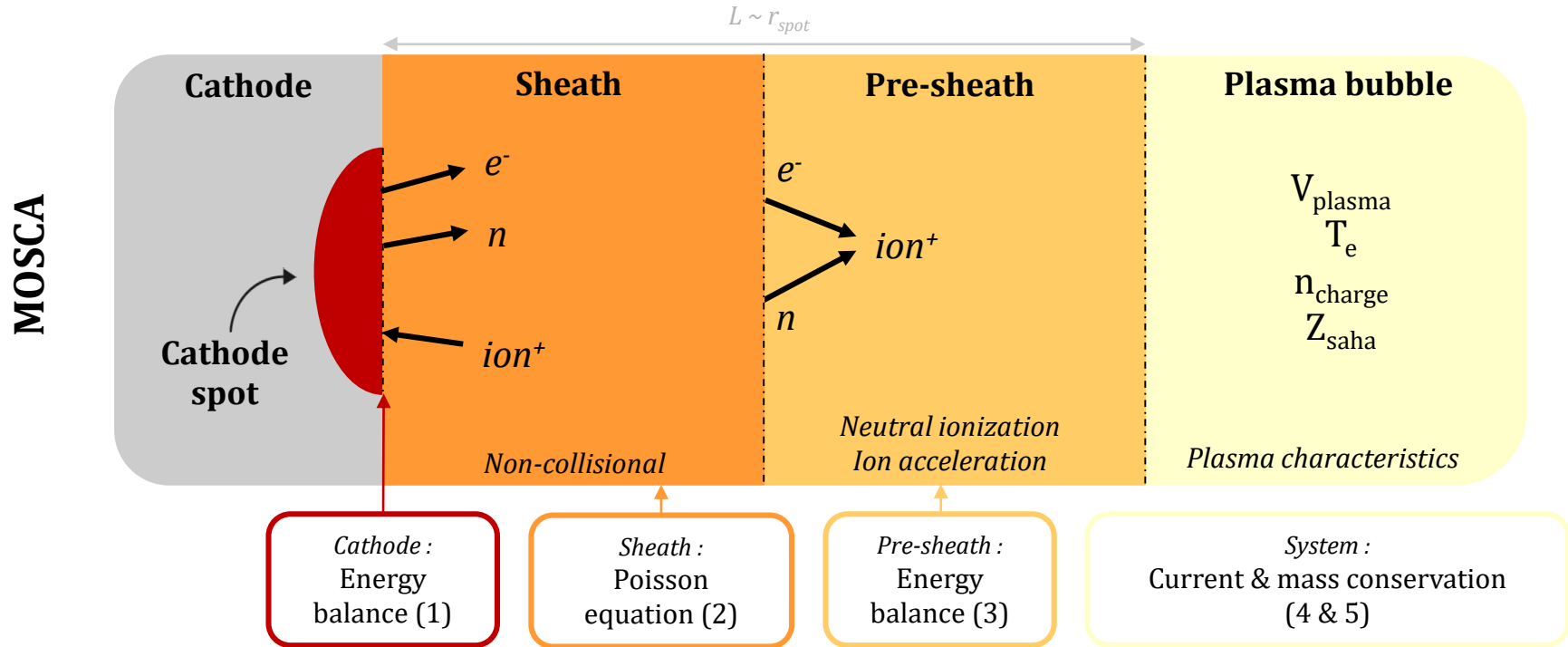
Structure of the coupled model



L. Monnin, S. Hess, J.-F. Roussel, P. Sarrailh, D. Payan, J. Appl. Phys. 130, 223302 (2021)

P. Sarrailh et al., IEEE Trans. Plasm. Sci. 41, 12 (2013)

Numerical model – Cathode spot model structure



L. Monnin, S. Hess, J.-F. Roussel, P. Sarrailh, D. Payan, J. Appl. Phys. 130, 223302 (2021)

Numerical model – Cathode spot model

Characteristics of the cathode spot model

Input parameters :

Spot size a
Cathode spot material
Initial charging state of panel

Equations :

Current conservation
Amount of substance conservation
Energy balance on the cathode
Energy balance in the pre-sheath
Poisson equation in the sheath

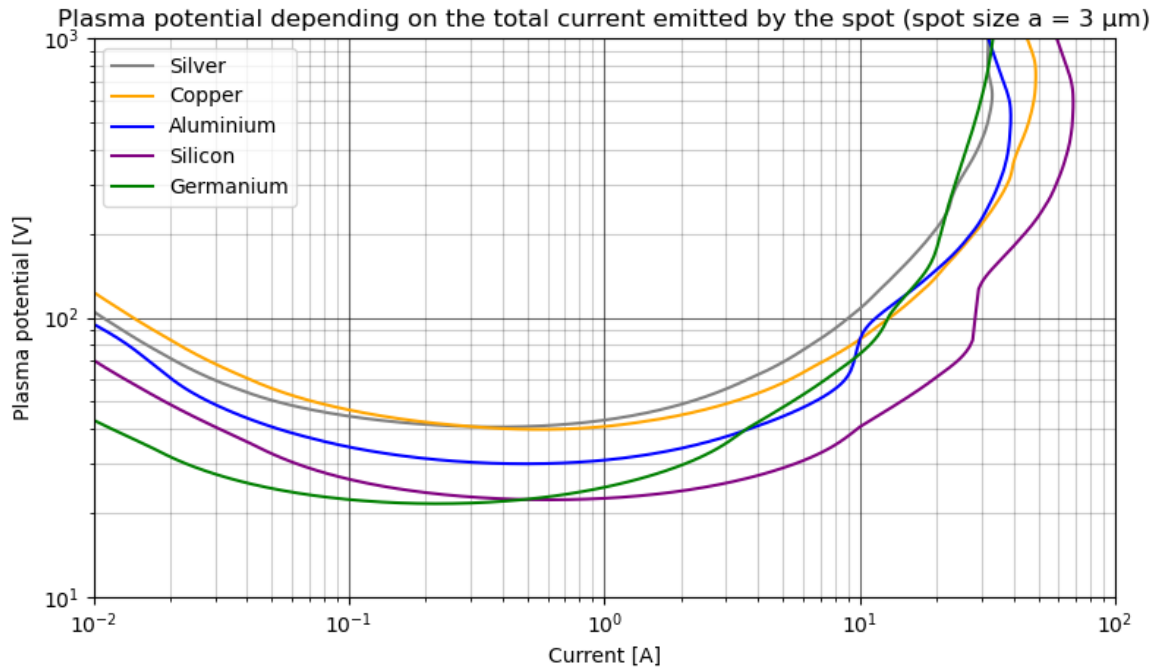
Computed quantities :

$\left\{ \begin{array}{l} I \\ T_s \\ E_s \\ V_g \\ T_e \end{array} \right\}$ Current emitted by the spot
Spot temperature
Electric field at the surface
Sheath potential drop
Electron temperature in the plasma

stationary solutions

Numerical model – Cathode spot model results

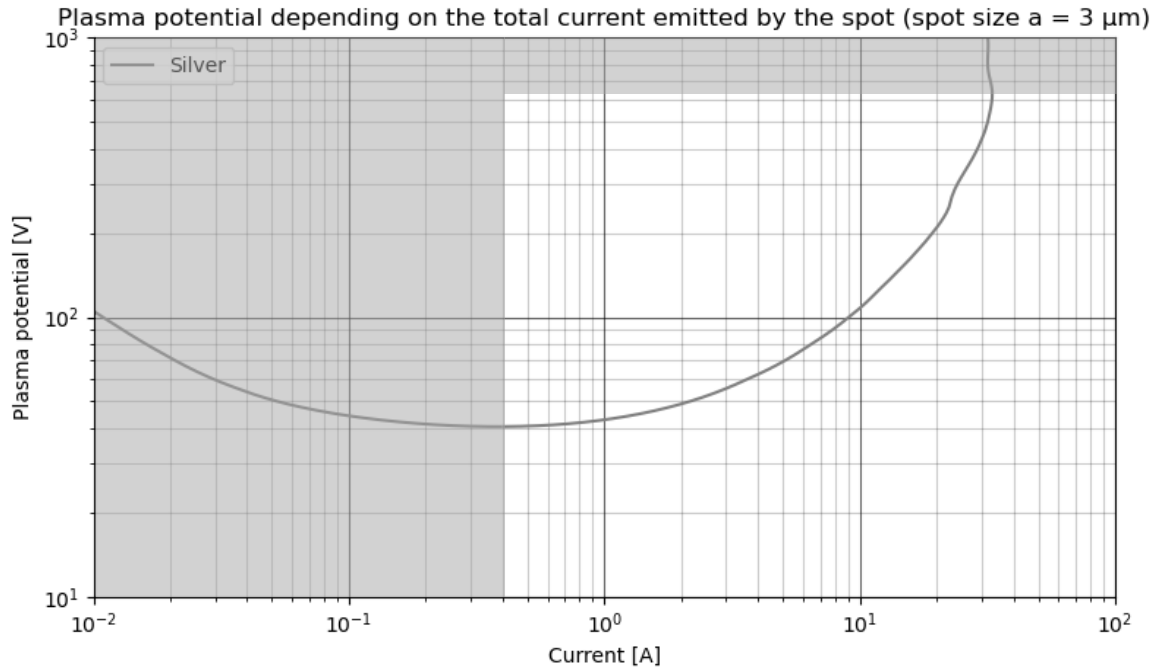
Output of MOSCA : **Plasma potential** function of spot current



➤ All materials have the **same variations**

Numerical model – Cathode spot model results

Output of MOSCA : **Plasma potential** function of spot current

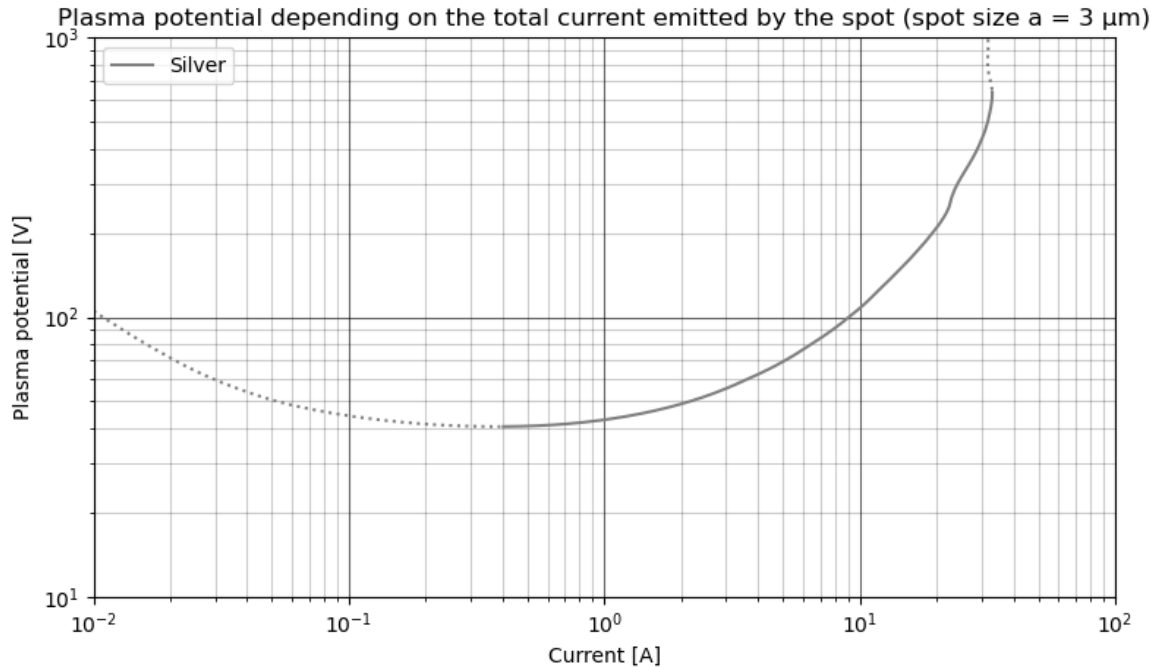


- All materials have the same variations
- Focus on Silver
 - ↳ Only the solutions described by the **increasing portion** of each curve are **stable** :

$$\frac{\partial I}{\partial V} > 0 \text{ in the model}$$

Numerical model – Cathode spot model results

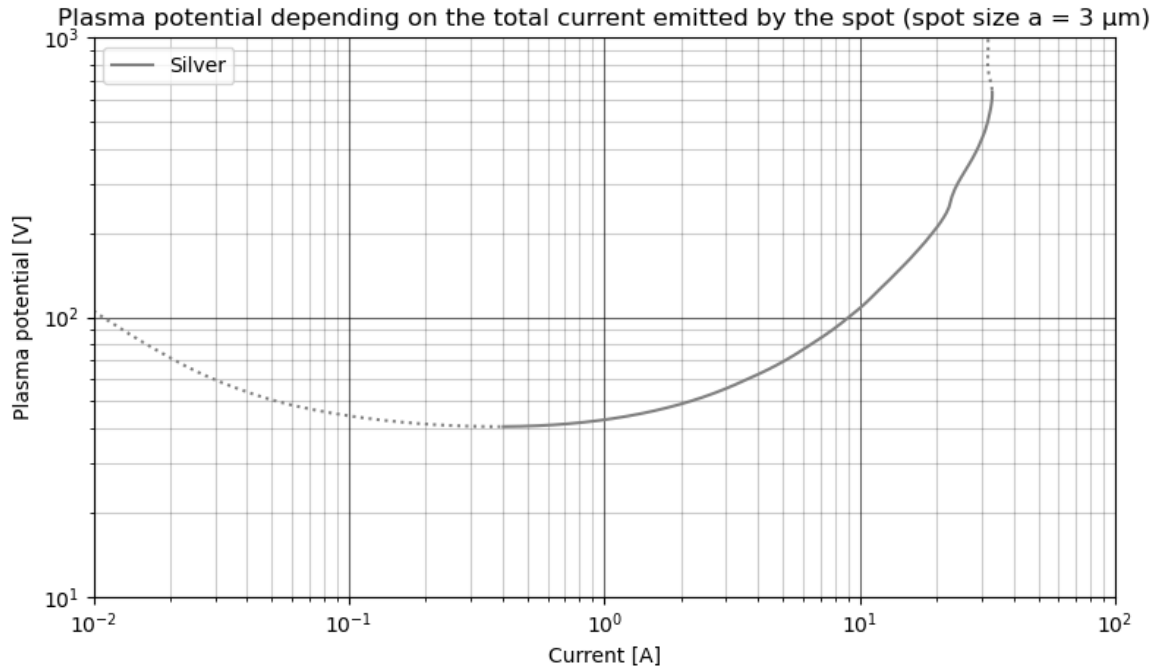
Output of MOSCA : **Plasma potential** function of spot current



- All materials have the same variations
- Focus on Silver
 - ↳ Only the solutions described by the increasing portion of each curve are stable
- Existence of tuple (I_{\min}, V_{\min})
 - ↳ **threshold values** for plasma emission hence for **spot existence**

Numerical model – Cathode spot model results

Output of MOSCA : **Plasma potential** function of spot current



- All materials have the same variations
- Focus on Silver
 - ↳ Only the solutions described by the increasing portion of each curve are stable
- Existence of tuple (I_{\min}, V_{\min})
 - ↳ **threshold values** for plasma emission hence for **spot existence**

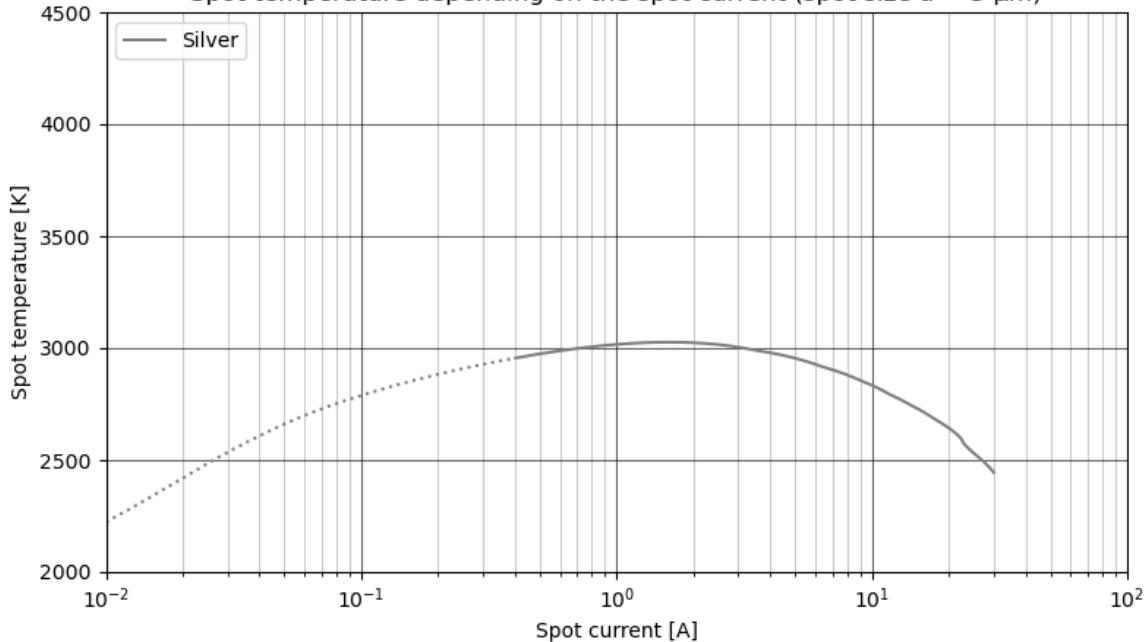
ESD current : ~ 0.5 to 10 A \longleftrightarrow Plasma potential : 40 to 100 V

↳ Consistent with observations

Numerical model – Cathode spot model results

Output of MOSCA : **Spot temperature** function of spot current

Spot temperature depending on the spot current (spot size $a = 3 \mu\text{m}$)



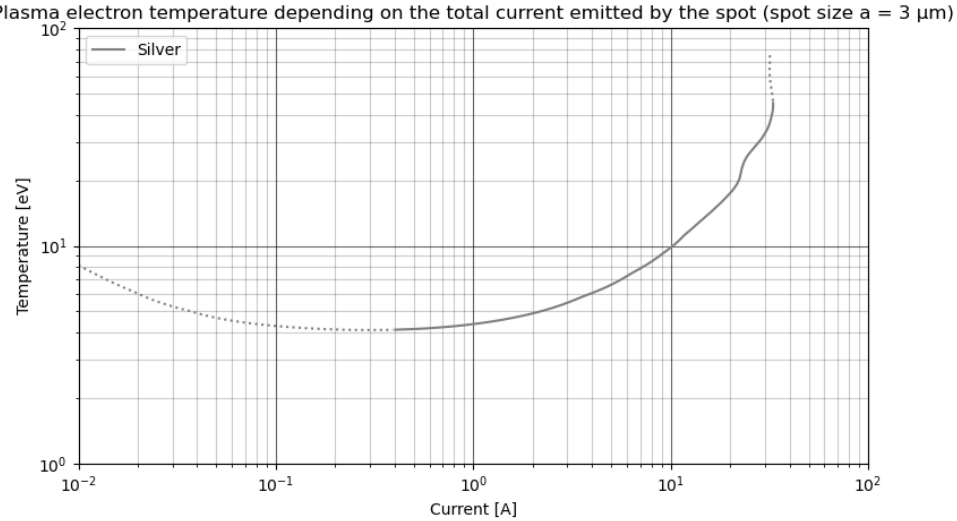
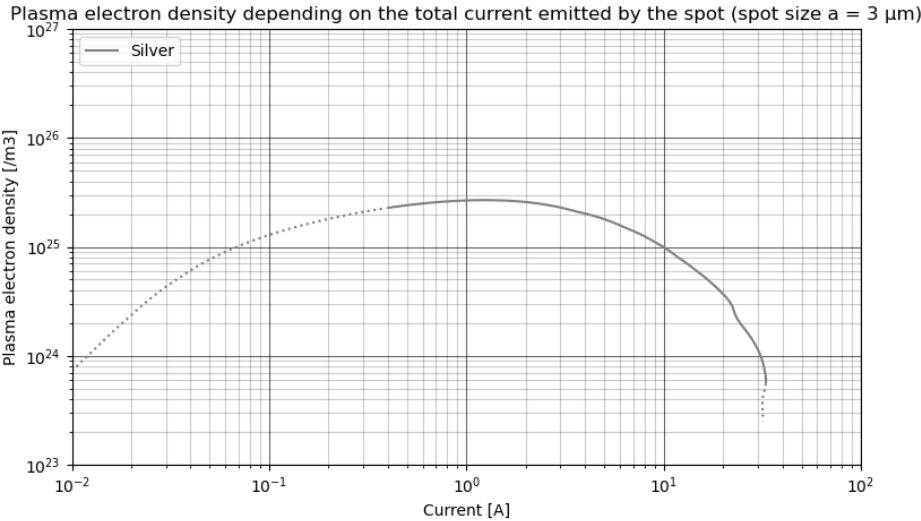
- All materials have the same variations
- Non monotonous curves
 - ↳ maximum value of 3000 K (at ~ 1.6 A)
 - ↳ after the peak value, spot **cooled down by the emission current** which consumes a lot of electron

ESD current : **1 to 10 A** ↔ Surface temperature : **~ 3000 K**

Numerical model – Cathode spot model results

Electron density in plasma function of spot current

Electron temperature in plasma function of spot current



➤ Same variations as spot surface temperature

↳ $n_g = A T_s^\alpha \sqrt{\frac{T_s}{T_e}}, \alpha > 0$ $n_e : \sim 10^{25} / \text{m}^3$

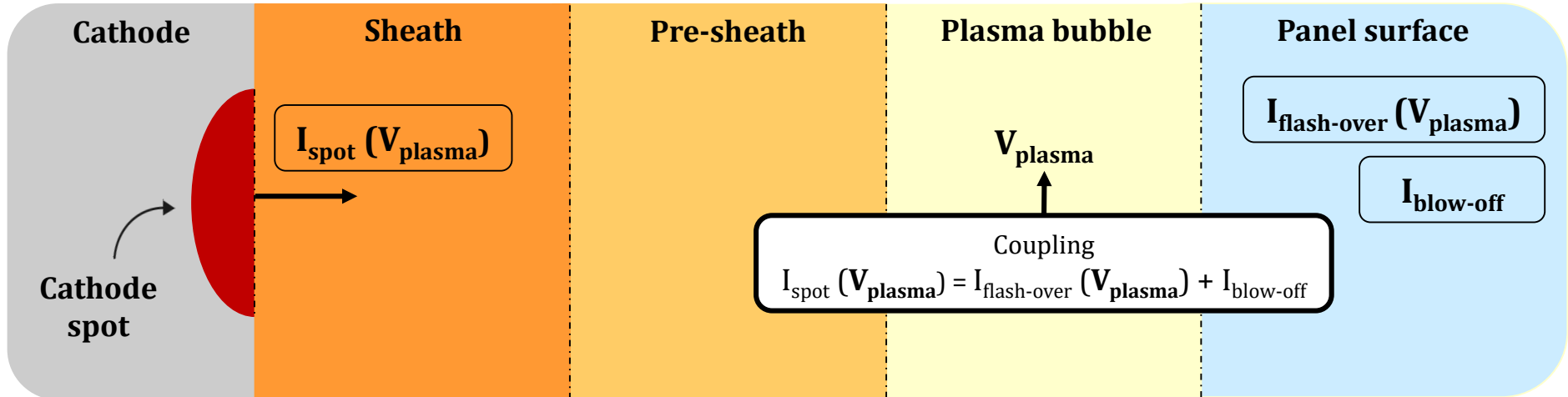
➤ Same variations as plasma and sheath potential

↳ V_g conditions the energy of charged particles

$T_e : 4 \text{ to } 10 \text{ eV}$

Numerical model – Electrostatic discharge global model

Structure of the coupled model



MOSCA : cathode spot model

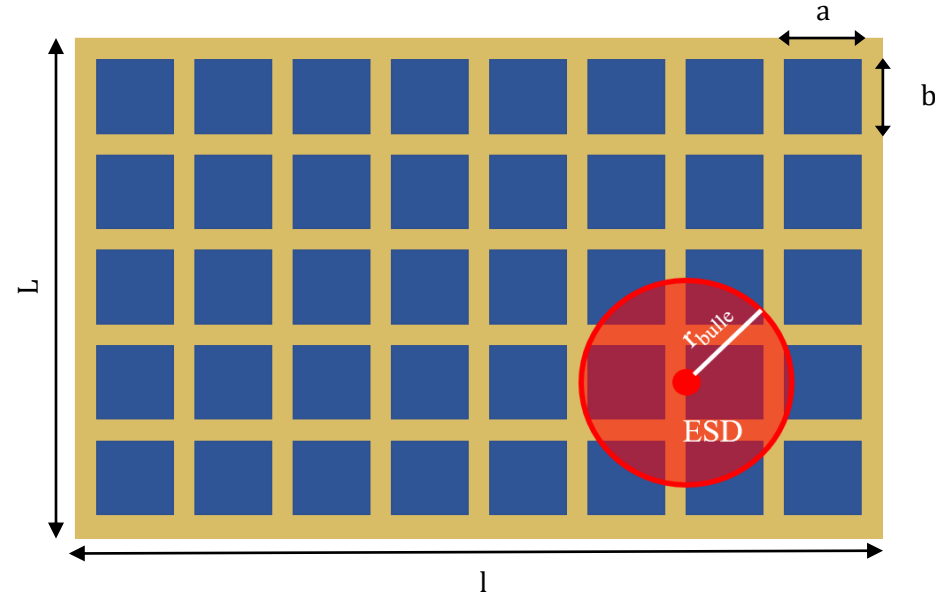
FOEBUS : plasma bubble expansion
& dielectric neutralization

] L. Monnin, S. Hess, J.-F. Roussel, P. Sarrailh, D. Payan, J. Appl. Phys. 130, 223302 (2021)
P. Sarrailh et al., IEEE Trans. Plasm. Sci. 41, 12 (2013)

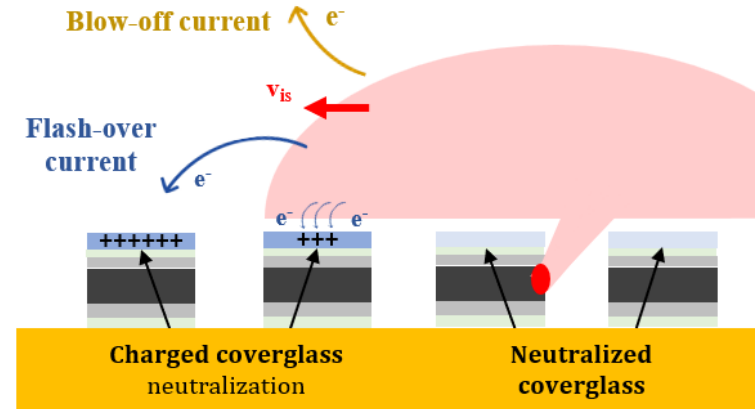
Numerical model – Bubble expansion model FOEBUS

FOEBUS

Flash-Over Bubble Simulator



Computation of collected current

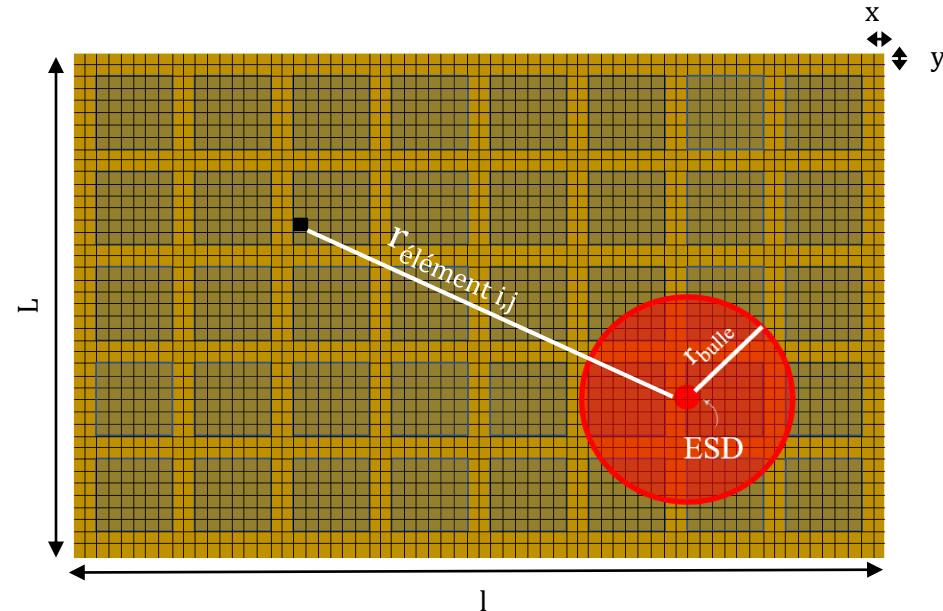


P. Sarrailh et al., IEEE Trans. Plasm. Sci. 41, 12 (2013)

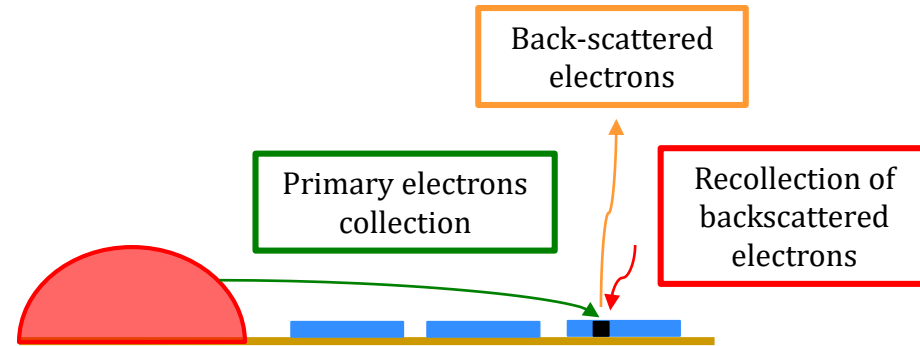
Numerical model – Bubble expansion model FOEBUS

FOEBUS

Flash-Over Bubble Simulator



Computation of collected current



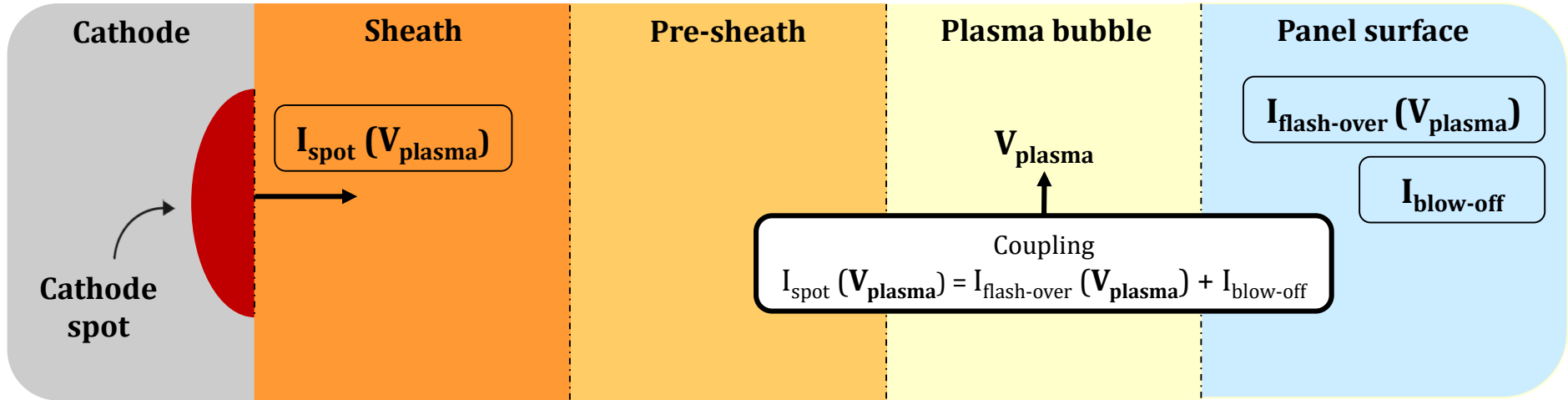
$$I_{i,j}(V_{i,j}(t - dt)) = I_{pe} - I_{bse} + I_{bsr}$$

$$V_{i,j}(t) = V_{i,j}(t - dt) - \frac{I_{i,j} dt}{c_{diel} dS}$$

The flash-over current is computed as a function of the plasma potential $\rightarrow I_{\text{flash-over}}(V_{\text{plasma}}) + I_{\text{blow-off}}$

Numerical model – Bubble expansion model FOEBUS

Structure of the coupled model



MOSCA : cathode spot model

FOEBUS : plasma bubble expansion
& dielectric neutralization

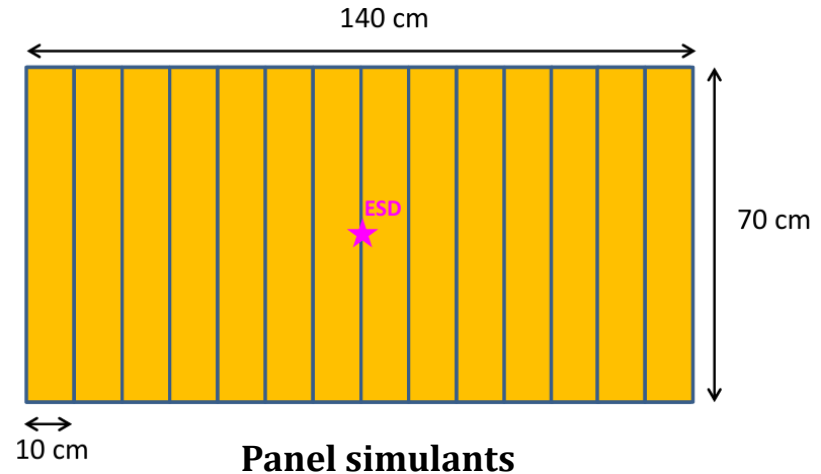
] L. Monnin, S. Hess, J.-F. Roussel, P. Sarrailh, D. Payan, J. Appl. Phys. 130, 223302 (2021)
P. Sarrailh et al., IEEE Trans. Plasm. Sci. 41, 12 (2013)

Test campaign : EMAGS 4 (ESA)

Length : **140 cm**
Width : **70 cm**
ESD : **Center**
Spot : **Aluminium / Silver**

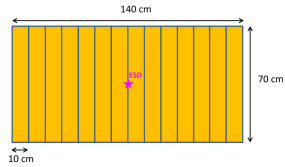
Numerical curve features

- Shape of flash-over current
- Duration of flash-over
- Neutralized charge



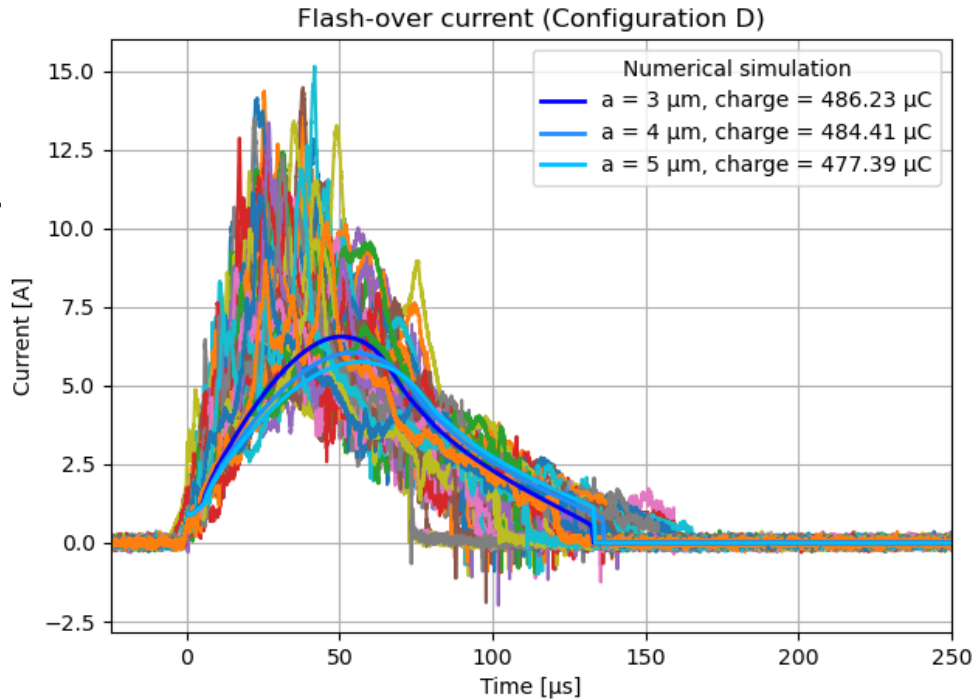
Results – Comparison with experimental results from EMAGS 4

Length : 140 cm
Width : 70 cm
ESD : Center
Spot : Aluminium



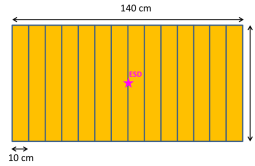
Numerical curve features

- Neutralized charge
- Shape
- Duration



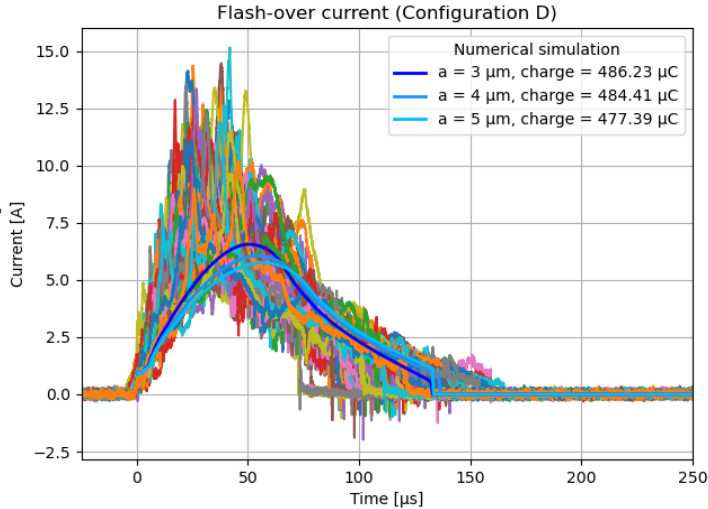
Results – Comparison with experimental results from EMAGS 4

Length : 140 cm
Width : 70 cm
ESD : Center
Spot : Aluminium



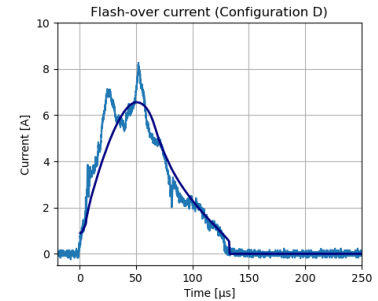
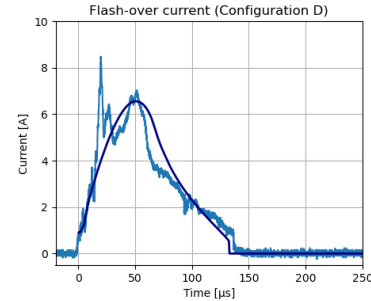
Numerical curve features

- Shape
- Duration
- Neutralized charge



- Satisfying shape of the curve
- Optimal spot radius : a = 3 μ m

Curve-to-curve comparison (3 μ m)



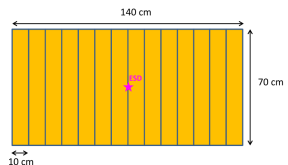
Results – Comparison with experimental results from EMAGS 4

Length : 140 cm

Width : 70 cm

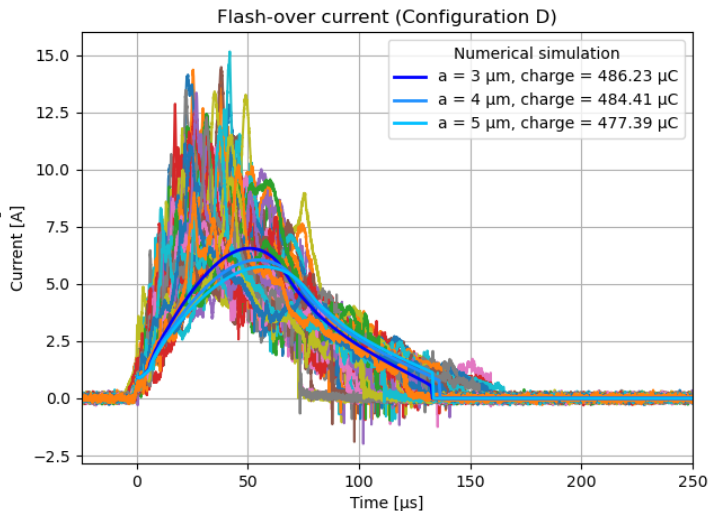
ESD : Center

Spot : Aluminium



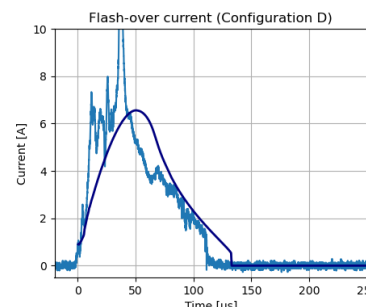
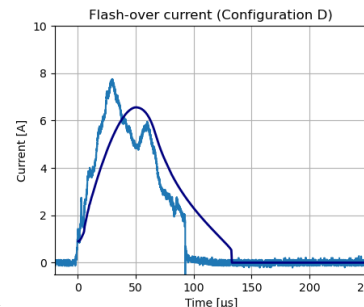
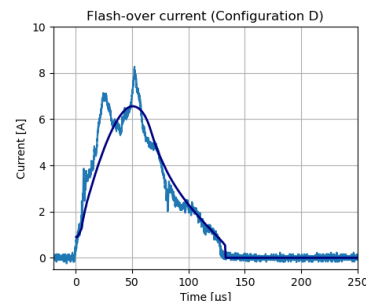
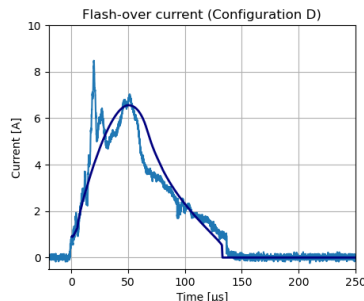
Numerical curve features

- Shape
- Duration
- Neutralized charge



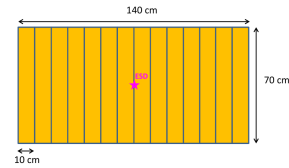
- Satisfying shape of the curve
- Optimal spot radius : $a = 3 \mu\text{m}$
- Estimation of τ_{ESD} and $I_{\text{cut-off}}$: upper bounds
 - Instabilities not taken into account
 - Simple cut-off condition : $V_{\text{bubble}} < V_{\text{min plasma}}$

Curve-to-curve comparison (3 μm)



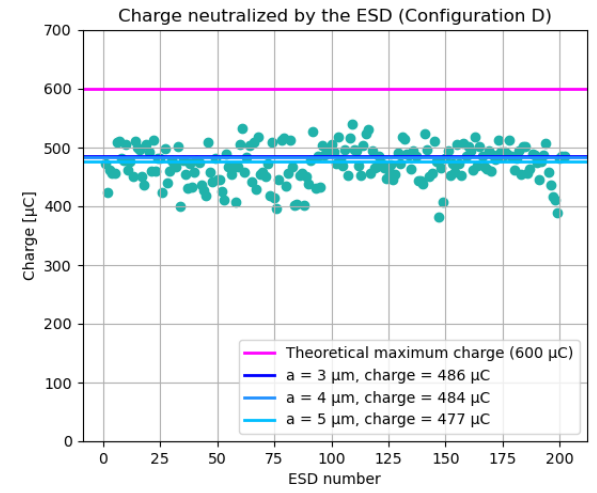
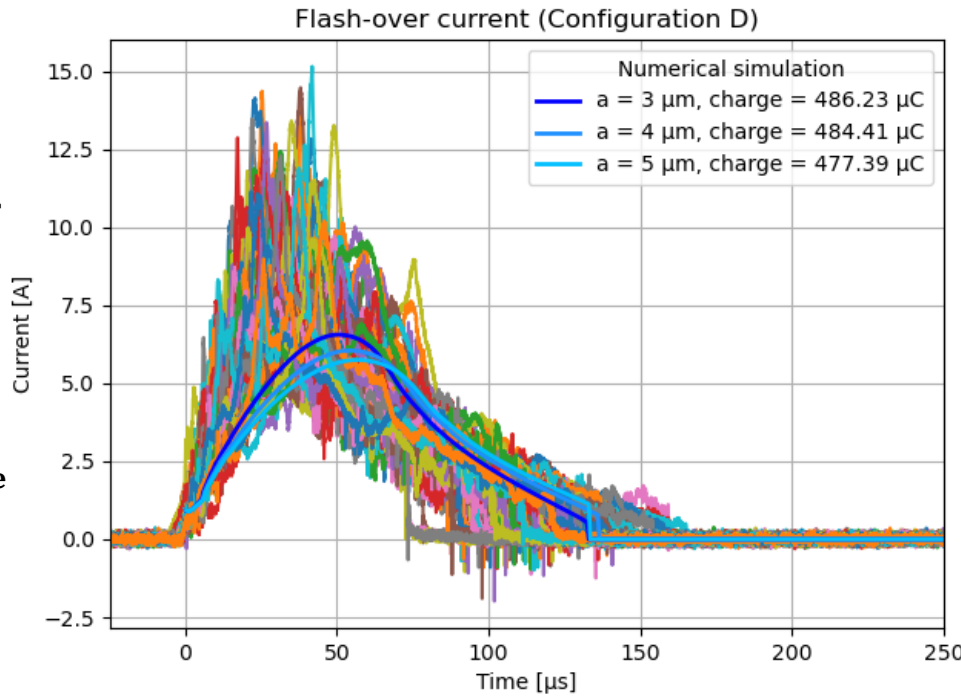
Results – Comparison with experimental results from EMAGS 4

Length : 140 cm
Width : 70 cm
ESD : Center
Spot : Aluminium



Numerical curve features

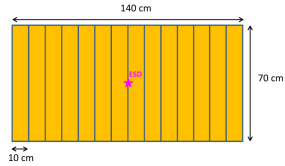
- Shape
- Duration
- Neutralized charge



- Good estimate of the experimental values

Results – Comparison with experimental results from EMAGS 4

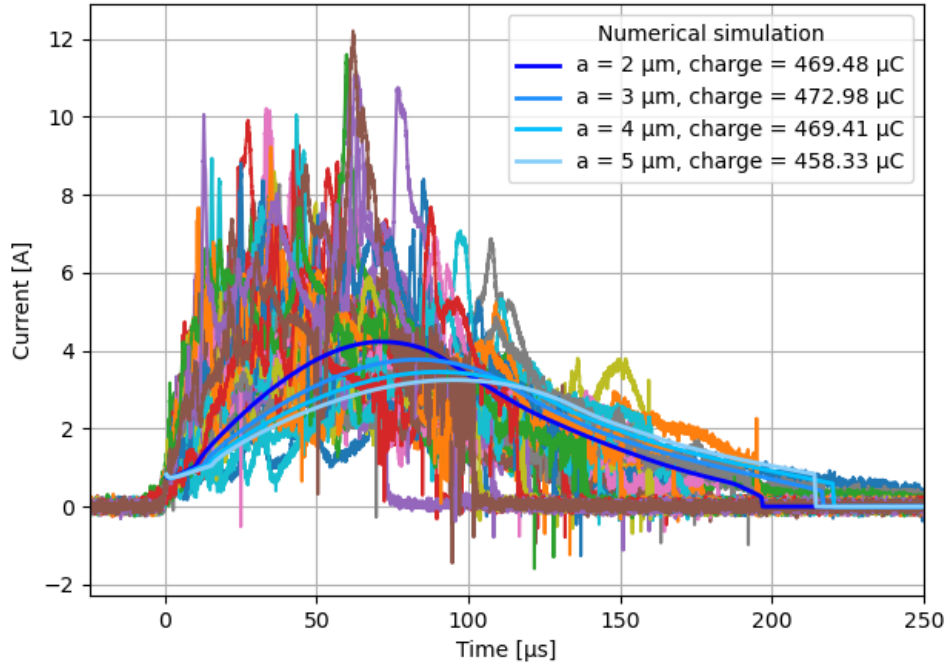
Length : 140 cm
Width : 70 cm
ESD : Center
Spot : Silver



Numerical curve features

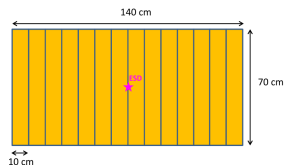
- Neutralized charge
- Shape
- Duration

Flash-over current (Configuration A)



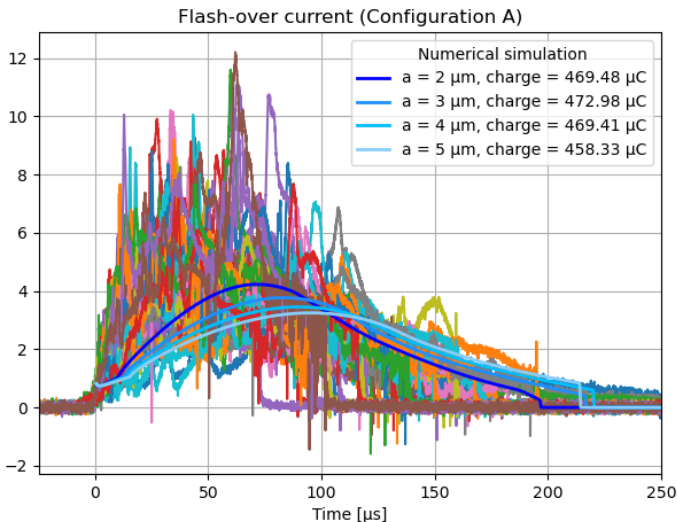
Results – Comparison with experimental results from EMAGS 4

Length : 140 cm
 Width : 70 cm
 ESD : Center
 Spot : Silver



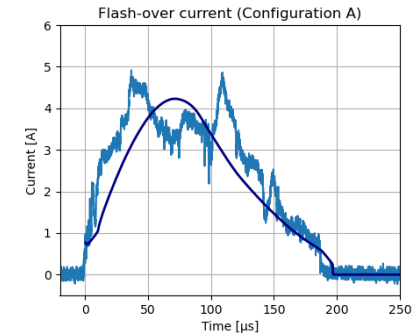
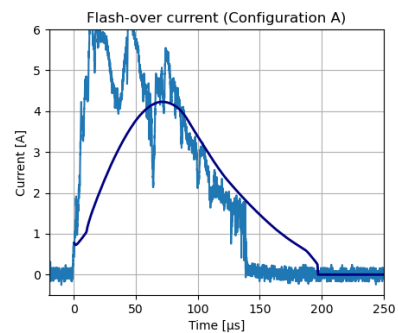
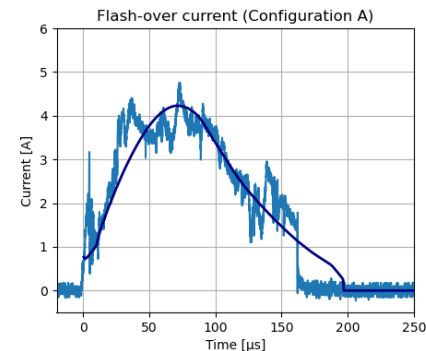
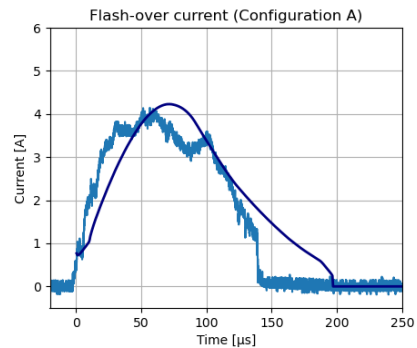
Numerical curve features

- Shape
- Duration
- Neutralized charge



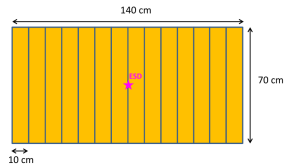
- Satisfying shape of the curve
- Optimal spot radius : $a = 2 \mu\text{m}$

Curve-to-curve comparison (2 μm)



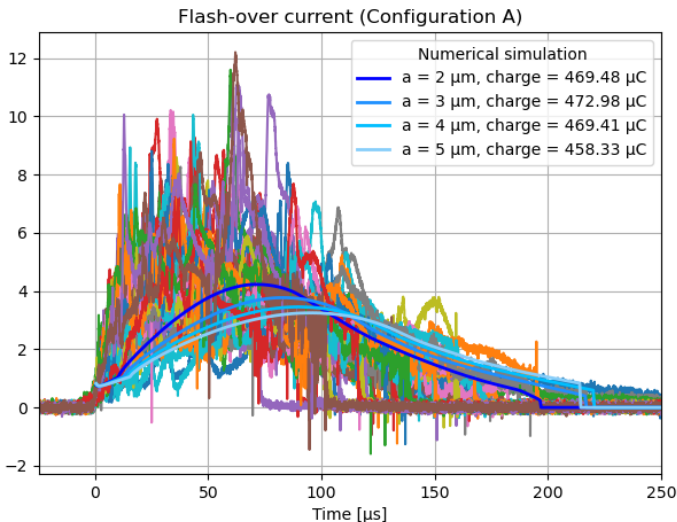
Results – Comparison with experimental results from EMAGS 4

Length : 140 cm
 Width : 70 cm
 ESD : Center
 Spot : Silver



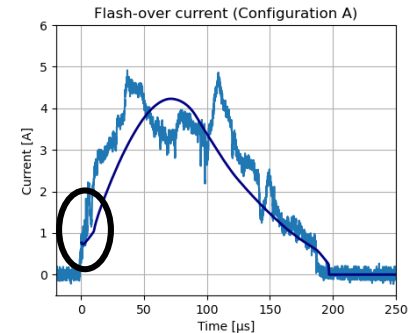
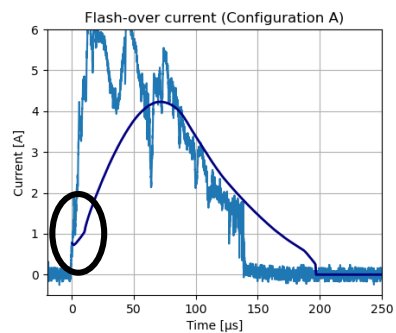
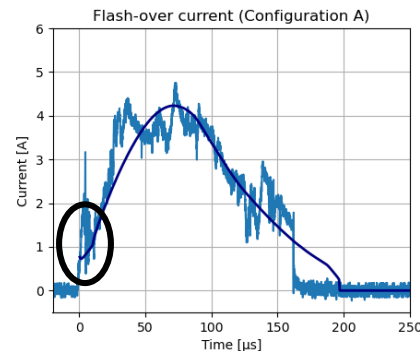
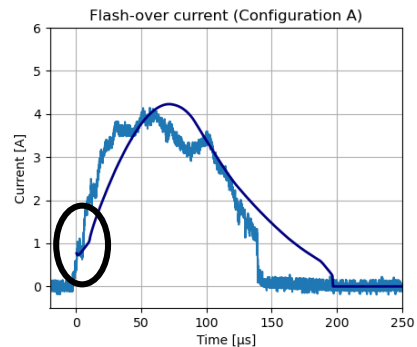
Numerical curve features

- Shape
- Duration
- Neutralized charge



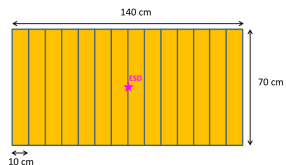
- Satisfying shape of the curve
- Optimal spot radius : $a = 2 \mu\text{m}$
- **Rising edge** of the numerical simulation is **slower** than most experimental curves

Curve-to-curve comparison ($2 \mu\text{m}$)



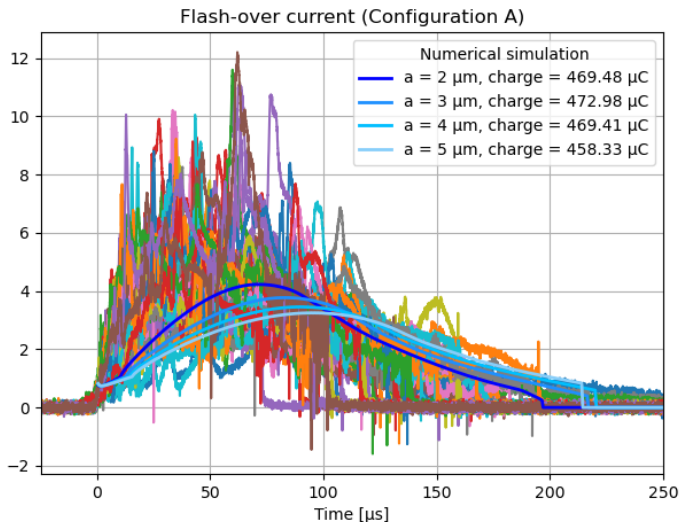
Results – Comparison with experimental results from EMAGS 4

Length : 140 cm
Width : 70 cm
ESD : Center
Spot : Silver



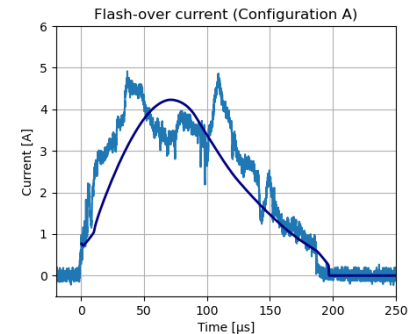
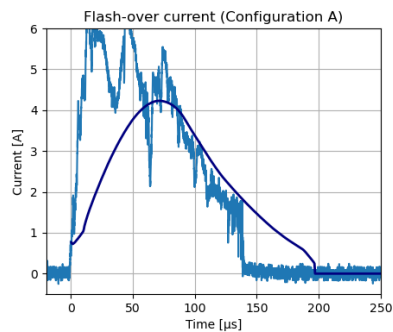
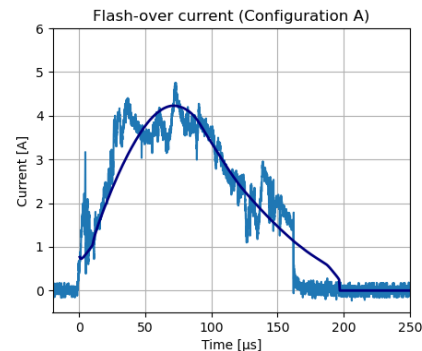
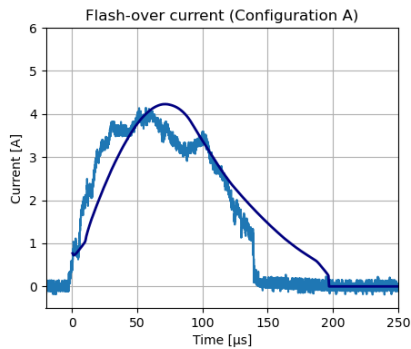
Numerical curve features

- Shape
- Duration
- Neutralized charge



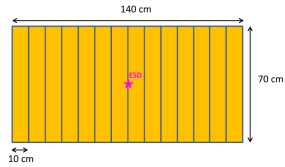
- Satisfying shape of the curve
- Optimal spot radius : $a = 2 \mu\text{m}$
- Rising edge of the numerical simulation is slower than most experimental curves
- **Poor estimate of the ESD duration & cut-off current**

Curve-to-curve comparison (2 μm)



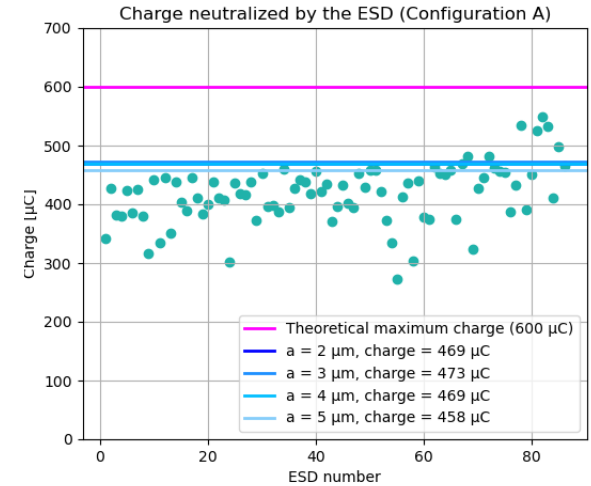
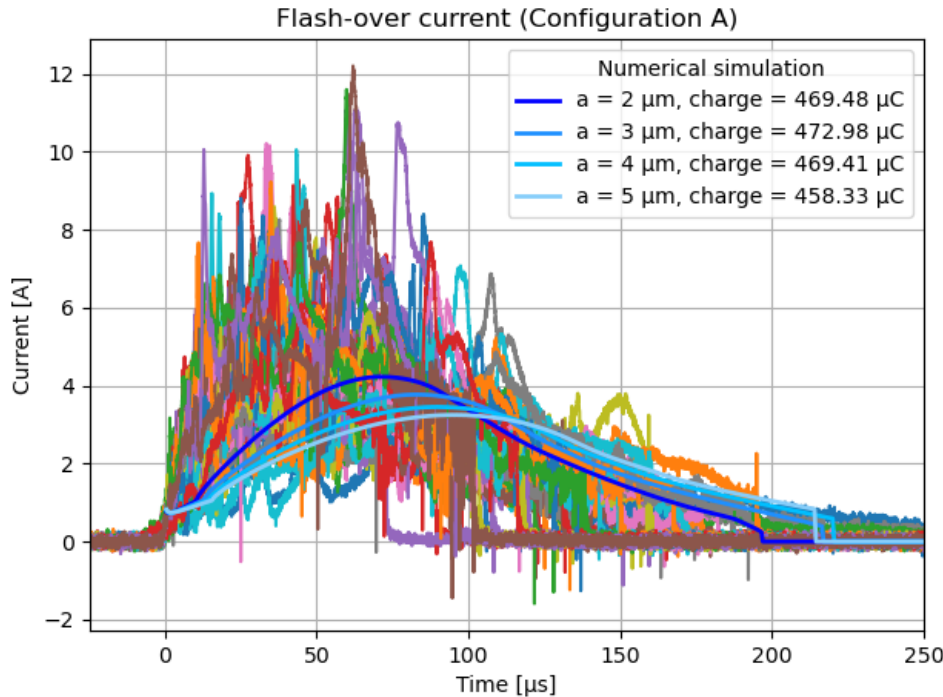
Results – Comparison with experimental results from EMAGS 4

Length : 140 cm
Width : 70 cm
ESD : Center
Spot : Silver



Numerical curve features

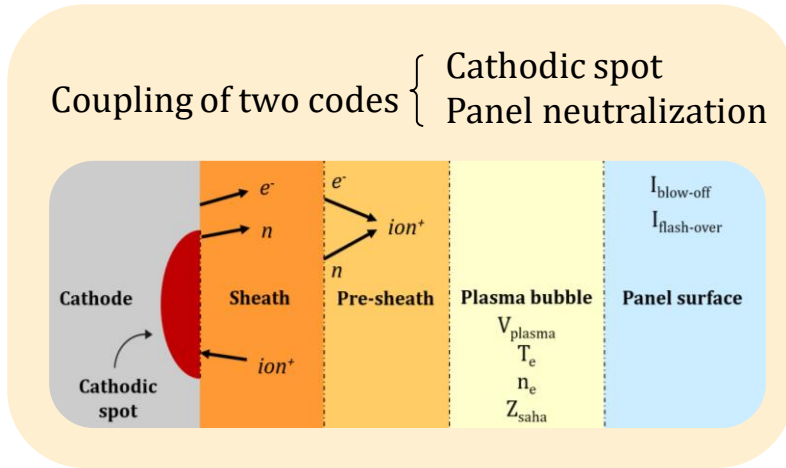
- Shape
- Duration
- Neutralized charge



- Charge neutralized by the simulations lies with the **high experimental values**

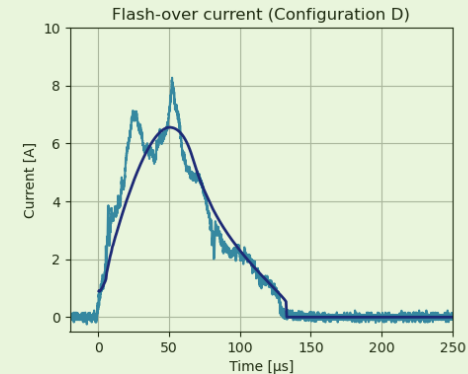
Conclusion

Numerical modelling of an electrostatic discharge on the solar panel of a satellite



- Main asset : only **1 free parameter**, the spot radius

Modelization of **flash-over current** for different configurations

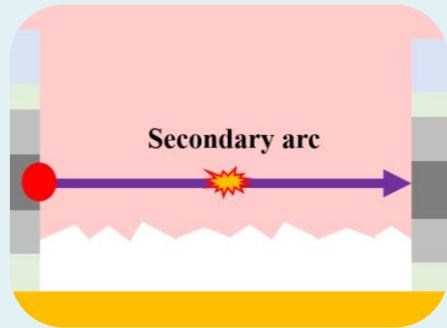


- Good estimate of neutralized charge & shape
- « Worst case scenario »

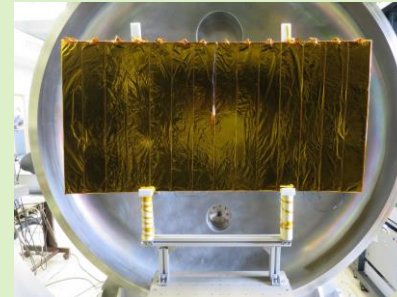
What's next ?

Numerical modelling of secondary arcing on the solar panel of a satellite

- Inspired of existing cathodic spot model
- Enrich it with **arc column** & **anodic phenomena**
- Consider **medium temperature** and material **degassing**
- **Coupling** between **primary** & **secondary arc** (at cathode scale)



Experimental campaign to test & validate the model



JONAS chamber (ONERA)

- Confirm LTE conditions
- Establish physical quantities of interest : T_e

How { Time-resolved optical emission spectrometry
↳ Spectrometer & streak camera



*Liberté
Égalité
Fraternité*



Thank you for your attention

Simulation of electric discharges on the solar panels of satellites

Capucine SOL¹, Sébastien Hess¹, Julien Jarrige¹, Carla Costa²

¹ONERA The French Aerospace Lab, DPHY/CSE, 2 ave M. Pélegrin 31400 Toulouse

²CNES, 18 Ave E. Belin 31400 Toulouse

Appendix A : MOSCA, the equations

Density of neutrals emitted by the spot

$$n_n = \frac{\alpha T_S^\beta}{k_B T_S} \exp\left(\frac{-\gamma}{T_S}\right)$$

Mean free path in pre-sheath

$$\Lambda_{col} = \frac{v_{th,e} m_e}{n_e e^2 \eta}, v_{th,e} = \sqrt{\frac{k_B T_e}{2 \pi m_e}}$$

Current density conservation

$$J = J_{e,cat} + J_{e,sec} + J_i - J_{e,pl}$$

$$J_{e,cat} = f(T_S, E_s) \text{ from Murhpy \& Good (Hantzsche version)}$$

$$J_{e,sec} = \gamma_{sec} \phi_i$$

$$J_i = Ze\phi_i$$

$$J_{e,pl} = e\phi_{e,pl}$$

With ϕ the current fluxes

Appendix A : MOSCA, the equations

Energy balance at the surface

$$S_{Joule} + S_{part\ on\ surf} = S_{cond} + S_{curr\ em} + S_{em\ part}$$

$$S_{Joule} = \rho(T_s) \frac{J^2 a}{12}$$

$$S_{part\ on\ surf} = \phi_{e,pl} 2k_B T_e + \phi_i (ZeV_g + Zk_B T_e + e\phi_i + W_{cd})$$

$$S_{cond} = \kappa \frac{T_s - T_{inf}}{a \ln\left(\frac{l}{a}\right)}$$

$$S_{curr\ em} = J\phi' \text{ (Current density modified by Schottky effect)}$$

$$S_{em\ part} = \phi_{cat} \cdot 2k_B T_s + \phi_{sec} \varepsilon_{sec} + \phi_n (2k_B T_s + W_{ev})$$

Appendix A : MOSCA, the equations

Energy balance in the pre-sheath

$$S_{Joule} + S_{neutrals} + S_{ionizing\ e} = S_{part\ leaving\ pre\ sheath} + S_{ionization\ energy}$$

$$S_{Joule} = \eta \frac{J^2 a}{12}, \eta \text{ the spitzer resistivity}$$

$$S_{neutrals} = \phi_n 2k_B T_s$$

$$S_{ionizing\ e} = \phi_n Z_g V_g$$

$$S_{curr\ em} = \phi_n ((2Z + Z_g) 2k_B T_e + 2Z k_B T_e)$$

$$S_{ionization} = \phi_n \sum \varphi_i$$

Mass conservation : $\phi_i = \phi_n$

$$n_n \sqrt{\frac{k_B T_s}{2\pi m_i}} = n_g \sqrt{\frac{k_B T_e}{2\pi m_i}}$$

Neutral emission outside the spot

Appendix A : MOSCA, the equations

Poisson's law in the pre-sheath

$$\int_0^{x_g} \frac{dE}{dx} E dx = -\frac{e}{\varepsilon_0} \int_0^{x_g} (Zn_i - n_e) \frac{d\varphi}{dx} dx$$



$$E_g^2 - E_s^2 = - \left. \begin{aligned} & \frac{J_i \sqrt{2\pi m_i}}{\pi Z e \varepsilon_0} \left(\sqrt{4\pi Z e \varphi_g + k_B T_e} - \sqrt{k_B T_e} \right) \\ & + \frac{(J_{cat} + J_{sec}) \sqrt{2\pi m_e}}{\pi e \varepsilon_0} \left(\sqrt{4\pi e \varphi_g + k_B T_s} - \sqrt{k_B T_s} \right) \\ & + \frac{2Z_{tot} n_g k_B T_e}{\varepsilon_0} \left(1 - \exp\left(\frac{-e\varphi_g}{k_B T_e}\right) \right) \end{aligned} \right\}$$

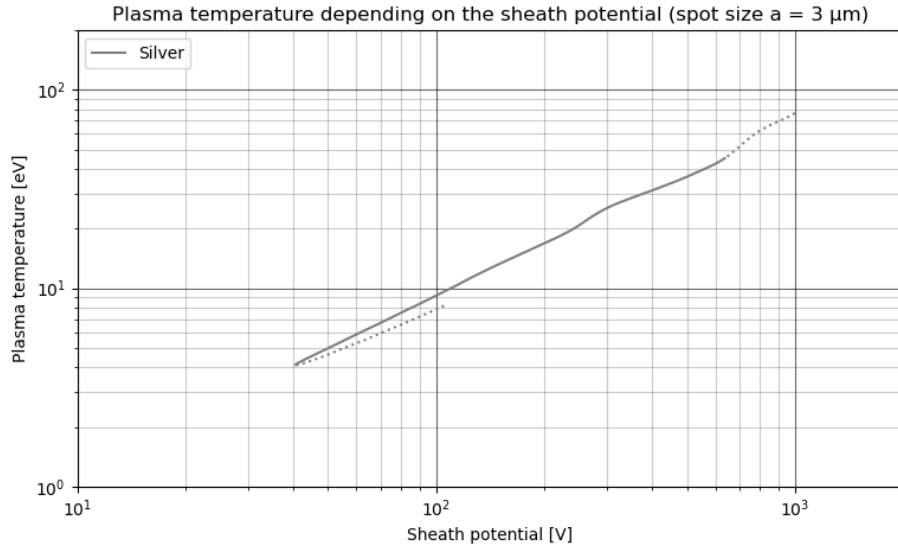
: ion density = $\frac{J_i}{v_i}$ where v_i is such as
 $m_i v_i^2 = 2e\varphi_g(x) + m_i v_{i,th}$

: electron density = $n_{cat} + n_{sec} + n_{rd}$

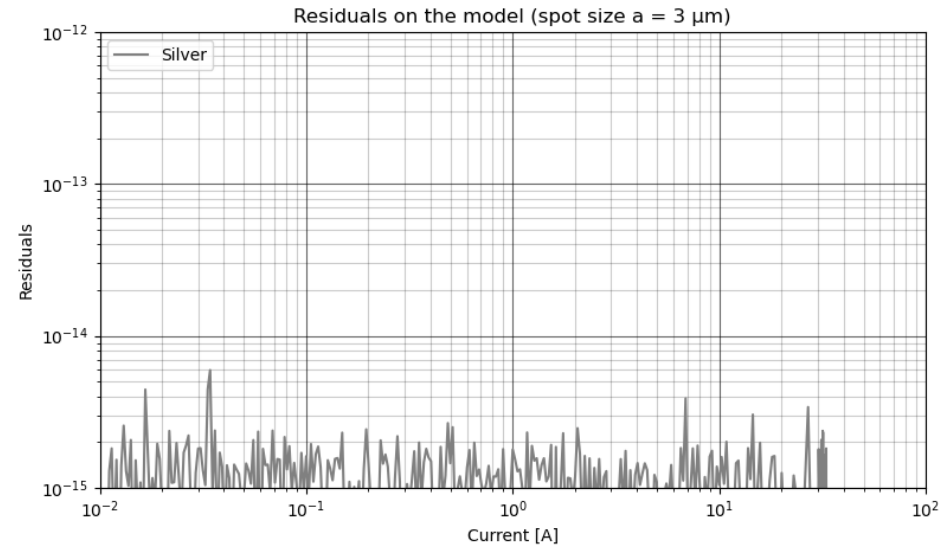
Same ballistic trajectory as ions Boltzmann distribution

Appendix A : MOSCA, other results

Plasma electronic temperature = $f(V_{\text{sheath}})$



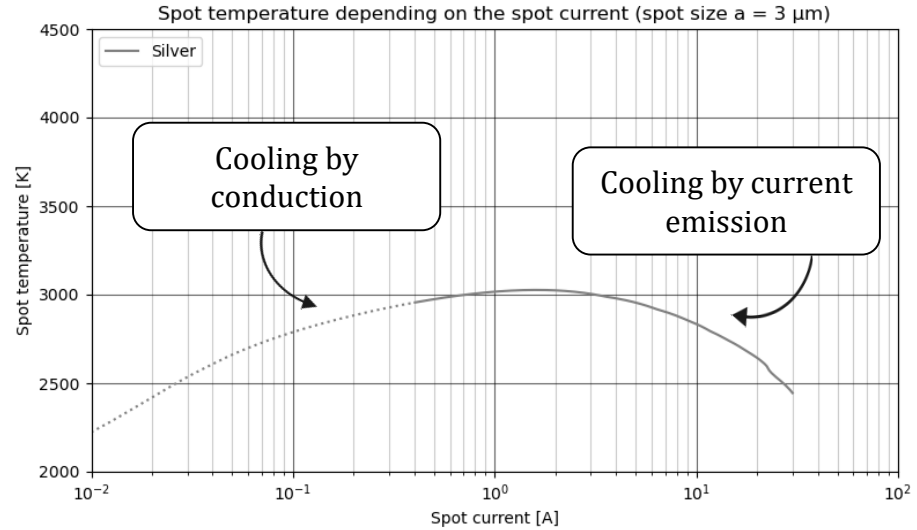
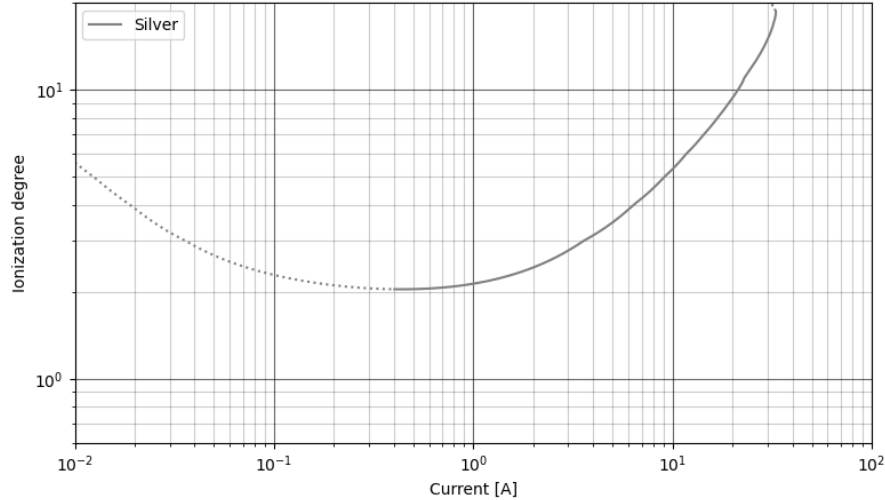
Residuals = $f(I_{\text{spot}})$



Appendix A : MOSCA, other results

Plasma ionization degree

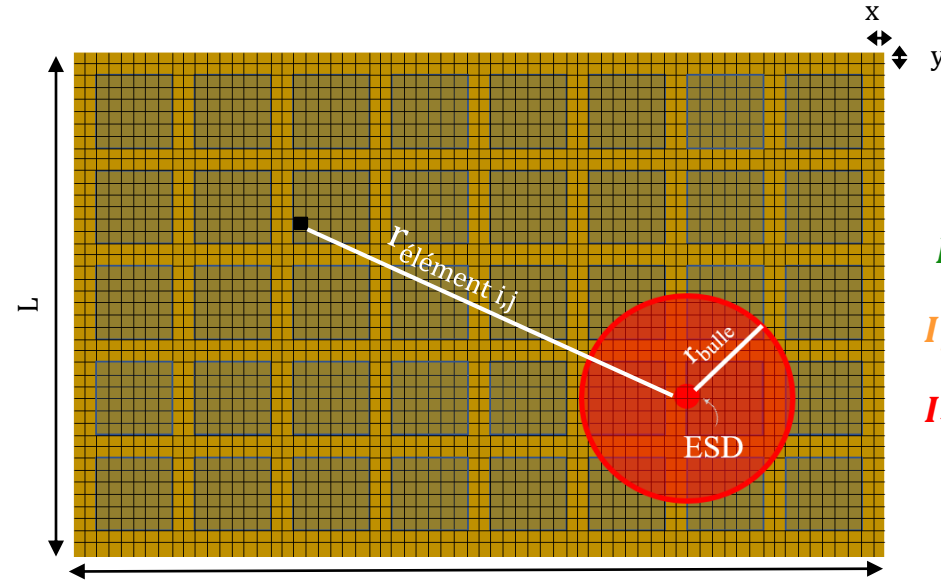
Plasma ionization degree depending on the total current emitted by the spot (spot size $a = 3 \mu\text{m}$)



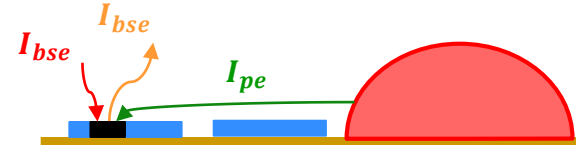
Appendix B : FOEBUS, current contributions in FO current

FOEBUS

Flash-Over Bubble Simulator



Computation of the collected current



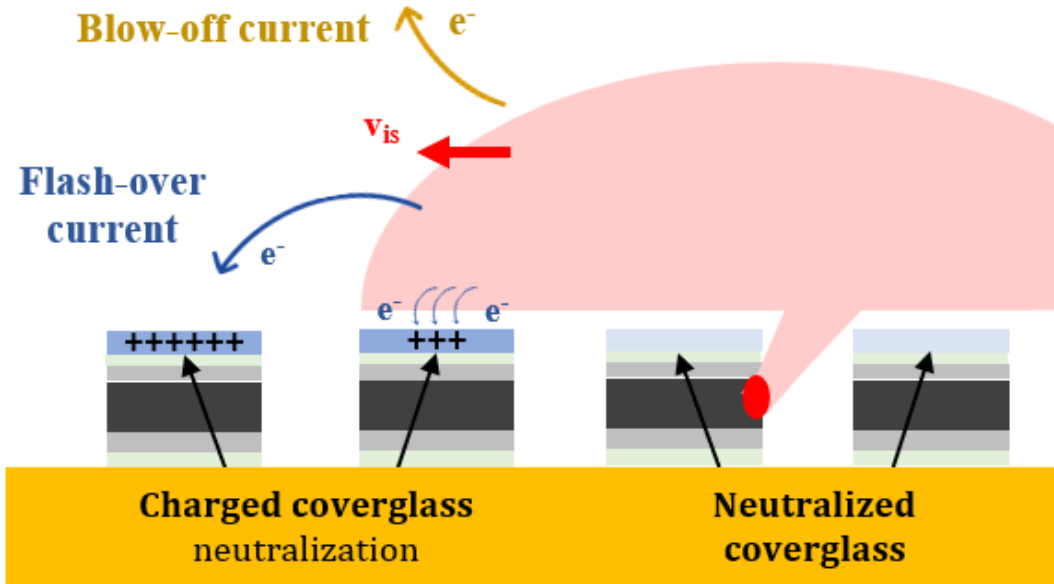
$$I_{i,j} = I_{pe} - I_{bse} + I_{rbs}$$

$$I_{pe} = \iint J_{Child-Langmuir} dS_{charged} dt + \frac{c_{diel} (V - v_B) dS_{neutralized}}{dt}$$

$$I_{bse} = \alpha I_{pe}, \alpha = 0.4$$

$$I_{rbs} = \beta e^{v/v_{max}}$$

Appendix B : FOEBUS, blow-off current



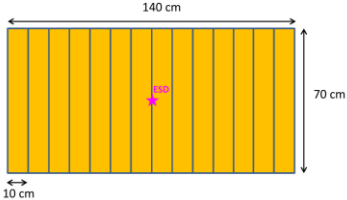
Computation of the blow-off current

$$I_{blow-off} = \frac{v_{sat} c_{sat}}{dt} \left(1 - \frac{1}{f^2} \right)$$

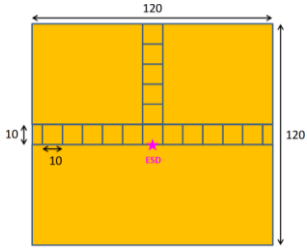
With $f(r_{bubble})$

Appendix C : EMAGS 4, experimental configurations

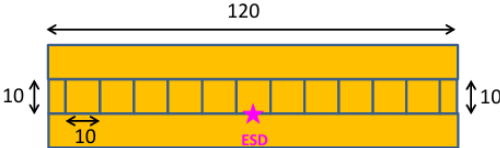
Configurations



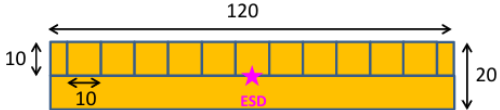
- 140 cm x 70 cm
- Aluminium
- Argent



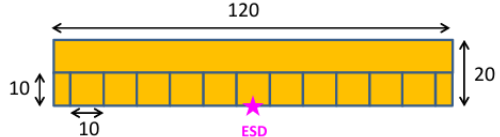
- 120 cm x 120 cm
- Aluminium
- Argent



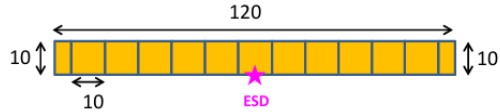
- 120 cm x 30 cm
- Aluminium



- 120 cm x 20 cm
- Aluminium



- 120 cm x 20 cm
- Aluminium



- 120 cm x 10 cm
- Aluminium